NUMERICAL SIMULATION OF STRUCTURAL CARBON STEEL, STAINLESS STEEL, AND INCONEL ALLOY 718 USING THE FINITE ELEMENT METHOD

Lukerman Douglas de Almeida[1] and Paulo Anderson Santana Rocha[2]
[1] Departamento de Engenharia Civil, Universidade Federal de Ouro Preto, Ouro Preto – MG, Brasil
lukermandouglas@yahoo.com.br
[2] Departamento de Engenharia Civil, Universidade Federal de Ouro Preto, Ouro Preto – MG, Brasil
paulorocha@ufop.edu.br

ABSTRACT

The aim of this work is the numerical analysis of structural carbon steel solid elements, including medium-strength steel (MS250) and high-strength steel (HS350), as well as 304 stainless steel (SS) and Inconel 718 superalloy (SI). To this end, a mathematical formulation based on the Finite Element Method (FEM) was implemented using the FORTRAN programming language. The aim was to obtain the values of stresses, strains and nodal displacements of the steels and the alloy, assuming that the materials had linear elastic behavior. The von Mises rupture criterion method was used to analyze the stresses. The solid elements were discretized using 4-node tetrahedral (T4) and 8-node hexahedral (H8) finite elements, with each node having three degrees of freedom. In addition, the Gauss-Legendre method (Gauss quadrature) was used to numerically solve the integrals. In order to verify and validate the results obtained with the computer program, comparisons were made with findings in the literature and then numerical analyses of the materials were carried out. The aim of this work is to make a significant contribution to the calculation of stresses, strains and displacements in solids.

KEYWORDS: *Finite Element Method, Numerical Analysis, Fortran, Gauss-Legendre Quadrature.*

I. INTRODUCTION

The application of computational tools for the resolution of structural analysis issues has witnessed a notable enhancement in efficacy. Since the 1950s, the utilisation of computational mechanics for the elucidation of extant phenomena in engineering has been progressively embraced.

Throughout history, engineers and mathematicians have developed a variety of methods to identify approximate solutions. The initial approaches were predicated on assumptions and simplifications that facilitated computations but often misrepresented the problem and yielded inaccurate solutions. With the advent of computers, the time and cost associated with performing a multitude of operations have been significantly reduced, thereby making numerical methods increasingly prevalent.

One of the analytical methods employed in numerous engineering research projects to address physical problems for which a mathematical model is represented by partial differential equations is the Finite Element Method (FEM).

Since 1967, numerous books have been published on the Finite Element Method, with notable contributions from Professor [1], [2], [3], [4], and [5]. During the same period, the method was extensively discussed in various academic journals.

It is noteworthy that the research conducted in this field includes the work of authors [6] and [7], who developed a computer program for the numerical analysis of three-dimensional problems using the finite element method. Their implementations yielded satisfactory results.

The objective of this research is to conduct a numerical mechanical analysis of solid elements pertaining to structural carbon steel (MS250 and HS350) and stainless steel (SS304), as well as inconel superalloy (SI718). These analyses will be conducted using numerical modeling of solid elements based on a computer program implemented in FORTRAN language [8], which is based on the Finite Element Method. The program will utilize two finite elements to model the problems: the 4-node tetrahedral finite element (T4) and the 8-node hexahedral finite element (H8).

Thus, the aim of this research is to obtain the values of stresses, deformations and displacements along the solids under study, in which these will be subjected to certain types of loads. In order to validate the numerical results obtained with the aid of the developed computer program, the answers will be compared with results found in the literature.

The article is divided into a brief introduction to the topic, then a presentation of the FEM formulations of the 4-node tetrahedral element and the 8-node hexahedral element, which were implemented in the computer program developed, then the applications, in which the modeling of the analyzed solids is presented in comparison with the literature, and finally the conclusion, in which the main results obtained with the analysis are described.

II. FORMULATIONS

Figure 1, shows the master elements of the 4-node tetrahedral finite element (T4) and 8-node hexahedral finite element (H8), respectively.

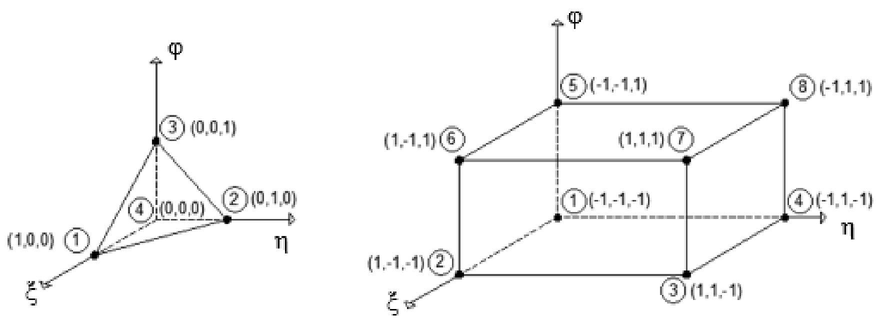

Figure 1 – Master elements

Next, the formulations of solid finite elements studied in this research are presented.

2.1 4-node Tetrahedral Finite Element

The shape functions corresponding to this element are:

$$N_1 = \xi \qquad N_2 = \eta \qquad N_3 = \varphi \tag{1}$$

$$N_1 + N_2 + N_3 + N_4 = 1 \tag{2}$$

The displacement vector will be described as:

$$q = [q_1 \quad q_2 \quad q_3 \quad q_4 \quad q_5 \quad q_6 \quad q_7 \quad q_8 \quad q_9 \quad q_{10} \quad q_{11} \quad q_{12}] \tag{3}$$

Being the relation between the vector of the field of displacements and the vector of nodal displacements given by:

$$\mathbf{u} = \mathbf{N}\ \mathbf{q} \tag{4}$$

Where N is the matrix representing the shape functions, given by:

$$\mathbf{N} = \begin{bmatrix} N_1 & 0 & 0 & N_2 & 0 & 0 & N_3 & 0 & 0 & N_4 & 0 & 0 \\ 0 & N_1 & 0 & 0 & N_2 & 0 & 0 & N_3 & 0 & 0 & N_4 & 0 \\ 0 & 0 & N_1 & 0 & 0 & N_2 & 0 & 0 & N_3 & 0 & 0 & N_4 \end{bmatrix} \tag{5}$$

Then, with the help of Eq. (4) and Eq. (5), it is possible to conclude that:

$$u = N_1 q_1 + N_2 q_4 + N_3 q_7 + N_4 q_{10} \tag{6}$$

$$v = N_1 q_2 + N_2 q_5 + N_3 q_8 + N_4 q_{11} \tag{7}$$

$$w = N_1 q_3 + N_2 q_6 + N_3 q_9 + N_4 q_{12} \tag{8}$$

Since the function u depends on x, y and z, and that these depend on the natural coordinates ξ, η and φ, then the function u is also dependent on ξ, η and φ. However, there is:

$$\begin{Bmatrix} \frac{\partial_u}{\partial_\xi} \\ \frac{\partial_u}{\partial_\eta} \\ \frac{\partial_u}{\partial_\varphi} \end{Bmatrix} = \begin{bmatrix} \frac{\partial_x}{\partial_\xi} & \frac{\partial_y}{\partial_\xi} & \frac{\partial_z}{\partial_\xi} \\ \frac{\partial_x}{\partial_\eta} & \frac{\partial_y}{\partial_\eta} & \frac{\partial_z}{\partial_\eta} \\ \frac{\partial_x}{\partial_\varphi} & \frac{\partial_y}{\partial_\varphi} & \frac{\partial_z}{\partial_\varphi} \end{bmatrix} \begin{Bmatrix} \frac{\partial_u}{\partial_x} \\ \frac{\partial_u}{\partial_y} \\ \frac{\partial_u}{\partial_z} \end{Bmatrix} \tag{9}$$

Since the Jacobian matrix is given by:

$$\mathbf{J} = \begin{bmatrix} \frac{\partial_x}{\partial_\xi} & \frac{\partial_y}{\partial_\xi} & \frac{\partial_z}{\partial_\xi} \\ \frac{\partial_x}{\partial_\eta} & \frac{\partial_y}{\partial_\eta} & \frac{\partial_z}{\partial_\eta} \\ \frac{\partial_x}{\partial_\varphi} & \frac{\partial_y}{\partial_\varphi} & \frac{\partial_z}{\partial_\varphi} \end{bmatrix} \tag{10}$$

Considering that the matrix **A** is the inverse matrix of the Jacobian matrix, it comes:

$$\mathbf{A} = \mathbf{J}^{-1} \tag{11}$$

Getting to:

$$\begin{Bmatrix} \frac{\partial_u}{\partial_x} \\ \frac{\partial_u}{\partial_y} \\ \frac{\partial_u}{\partial_z} \end{Bmatrix} = \mathbf{A} \begin{Bmatrix} \frac{\partial_u}{\partial_\xi} \\ \frac{\partial_u}{\partial_\eta} \\ \frac{\partial_u}{\partial_\varphi} \end{Bmatrix} \tag{12}$$

We have that the relation between the strain vector and the displacement vector is:

$$\boldsymbol{\varepsilon} = \mathbf{B}\,\mathbf{q} \tag{13}$$

Knowing that the strain vector is defined by:

$$\boldsymbol{\varepsilon} = [\varepsilon_x \quad \varepsilon_y \quad \varepsilon_z \quad \gamma_{zy} \quad \gamma_{zx} \quad \gamma_{yx}]^T \tag{14}$$

After some mathematical manipulations it is possible to conclude that the matrix **B** is equal to:

$$\mathbf{B} = \begin{bmatrix} A_{11} & 0 & 0 & A_{12} & 0 & 0 & A_{13} & 0 & 0 & -\tilde{A}_1 & 0 & 0 \\ 0 & A_{21} & 0 & 0 & A_{22} & 0 & 0 & A_{23} & 0 & 0 & -\tilde{A}_2 & 0 \\ 0 & 0 & A_{31} & 0 & 0 & A_{32} & 0 & 0 & A_{33} & 0 & 0 & -\tilde{A}_3 \\ 0 & A_{31} & A_{21} & 0 & A_{12} & A_{22} & 0 & A_{33} & A_{23} & 0 & -\tilde{A}_3 & -\tilde{A}_2 \\ A_{31} & 0 & A_{11} & A_{32} & 0 & A_{12} & A_{33} & 0 & A_{13} & -\tilde{A}_3 & 0 & -\tilde{A}_1 \\ A_{21} & A_{11} & 0 & A_{22} & A_{12} & 0 & A_{23} & A_{13} & 0 & -\tilde{A}_2 & -\tilde{A}_1 & 0 \end{bmatrix} \tag{15}$$

Given that:

$$-\tilde{A}_1 = [A_{11} + A_{12} + A_{13}] \tag{16}$$

$$-\tilde{A}_2 = [A_{21} + A_{22} + A_{23}] \tag{17}$$

$$-\tilde{A}_3 = [A_{31} + A_{32} + A_{33}] \tag{18}$$

The stiffness of the element can be obtained based on the internal strain energy equation, given by:

$$U_e = \frac{1}{2}\,\mathbf{q}^T\,\mathbf{B}^T\,\mathbf{D}\,\mathbf{B}\,\mathbf{q} \int_e dV \tag{19}$$

where the element stiffness matrix will be defined by:

$$\mathbf{k}_e = V_e\,\mathbf{B}^T\,\mathbf{D}\,\mathbf{B} \tag{20}$$

In turn, the body force (corresponding to its own weight) will be given by:

$$\mathbf{f_e} = \int_0^1 \int_0^{1-\xi} \int_0^{1-\xi-\eta} \mathbf{N}^T \, \mathbf{f} \, |det\, J| \, d\varphi \, d\eta \, d\xi \tag{21}$$

2.2 8-node Hexahedral Finite Element

The Lagrange shape functions are represented as:

$$N_i = \frac{1}{8} \ (1 + \xi_i \ \xi)(1 + \eta_i \ \eta)(1 + \varphi_i \ \varphi) \tag{22}$$

The element stiffness matrix corresponding to the hexahedral finite element with 8 nodes is defined as:

$$\mathbf{k^e} = \int_{-1}^1 \int_{-1}^1 \int_{-1}^1 \mathbf{B}^T \, \mathbf{D} \, \mathbf{B} \, |det\, J| \, d\varphi \, d\eta \, d\xi \tag{23}$$

Remembering that the integrals will be solved numerically with the aid of the Gauss-Legendre Method (Gauss Quadrature).
Considering that the gamma matrix is the inverse matrix of the Jacobian matrix, we have:

$$\mathbf{\Gamma} = \mathbf{J}^{-1} \tag{24}$$

Hence, it comes to:

$$\begin{Bmatrix} \dfrac{\partial_u}{\partial_x} \\ \dfrac{\partial_u}{\partial_y} \\ \dfrac{\partial_u}{\partial_z} \end{Bmatrix} = \mathbf{\Gamma} \begin{Bmatrix} \dfrac{\partial_u}{\partial_\xi} \\ \dfrac{\partial_u}{\partial_\eta} \\ \dfrac{\partial_u}{\partial_\varphi} \end{Bmatrix} \tag{25}$$

The matrix B corresponding to the hexahedral finite element is represented as:

$$\mathbf{B} = \mathbf{H} \ \ \mathbf{\Gamma_u} \ \mathbf{DN} \tag{26}$$

From Eq. (27) it is possible to conclude that:

$$\begin{bmatrix} \frac{\partial_u}{\partial_\xi} \\ \frac{\partial_u}{\partial_\eta} \\ \frac{\partial_u}{\partial_\varphi} \\ \frac{\partial_v}{\partial_\xi} \\ \frac{\partial_v}{\partial_\eta} \\ \frac{\partial_v}{\partial_\varphi} \\ \frac{\partial_w}{\partial_\xi} \\ \frac{\partial_w}{\partial_\eta} \\ \frac{\partial_w}{\partial_\varphi} \end{bmatrix} = \mathbf{DN}\ \ \mathbf{q} \tag{27}$$

since the DN matrix has 9 rows and 24 columns and will be organized using the sub-matrices proposed in this work and presented as:

$$\mathbf{DN1} = \begin{bmatrix} \frac{\partial_{N1}}{\partial_\xi} & 0 & 0 & \frac{\partial_{N2}}{\partial_\xi} & 0 & 0 \\ \frac{\partial_{N1}}{\partial_\eta} & 0 & 0 & \frac{\partial_{N2}}{\partial_\eta} & 0 & 0 \\ \frac{\partial_{N1}}{\partial_\varphi} & 0 & 0 & \frac{\partial_{N2}}{\partial_\varphi} & 0 & 0 \end{bmatrix} \tag{28}$$

$$\mathbf{DN2} = \begin{bmatrix} \frac{\partial_{N3}}{\partial_\xi} & 0 & 0 & \frac{\partial_{N4}}{\partial_\xi} & 0 & 0 \\ \frac{\partial_{N3}}{\partial_\eta} & 0 & 0 & \frac{\partial_{N4}}{\partial_\eta} & 0 & 0 \\ \frac{\partial_{N3}}{\partial_\varphi} & 0 & 0 & \frac{\partial_{N4}}{\partial_\varphi} & 0 & 0 \end{bmatrix} \tag{29}$$

$$\mathbf{DN3} = \begin{bmatrix} \frac{\partial_{N5}}{\partial_\xi} & 0 & 0 & \frac{\partial_{N6}}{\partial_\xi} & 0 & 0 \\ \frac{\partial_{N5}}{\partial_\eta} & 0 & 0 & \frac{\partial_{N6}}{\partial_\eta} & 0 & 0 \\ \frac{\partial_{N5}}{\partial_\varphi} & 0 & 0 & \frac{\partial_{N6}}{\partial_\varphi} & 0 & 0 \end{bmatrix} \tag{30}$$

$$\mathbf{DN4} = \begin{bmatrix} \frac{\partial_{N7}}{\partial_{\xi}} & 0 & 0 & \frac{\partial_{N8}}{\partial_{\xi}} & 0 & 0 \\ \frac{\partial_{N7}}{\partial_{\eta}} & 0 & 0 & \frac{\partial_{N8}}{\partial_{\eta}} & 0 & 0 \\ \frac{\partial_{N7}}{\partial_{\varphi}} & 0 & 0 & \frac{\partial_{N8}}{\partial_{\varphi}} & 0 & 0 \end{bmatrix} \tag{31}$$

$$\mathbf{DN5} = \begin{bmatrix} 0 & \frac{\partial_{N1}}{\partial_{\xi}} & 0 & 0 & \frac{\partial_{N2}}{\partial_{\xi}} & 0 \\ 0 & \frac{\partial_{N1}}{\partial_{\eta}} & 0 & 0 & \frac{\partial_{N2}}{\partial_{\eta}} & 0 \\ 0 & \frac{\partial_{N1}}{\partial_{\varphi}} & 0 & 0 & \frac{\partial_{N2}}{\partial_{\varphi}} & 0 \end{bmatrix} \tag{32}$$

$$\mathbf{DN6} = \begin{bmatrix} 0 & \frac{\partial_{N3}}{\partial_{\xi}} & 0 & 0 & \frac{\partial_{N4}}{\partial_{\xi}} & 0 \\ 0 & \frac{\partial_{N3}}{\partial_{\eta}} & 0 & 0 & \frac{\partial_{N4}}{\partial_{\eta}} & 0 \\ 0 & \frac{\partial_{N3}}{\partial_{\varphi}} & 0 & 0 & \frac{\partial_{N4}}{\partial_{\varphi}} & 0 \end{bmatrix} \tag{33}$$

$$\mathbf{DN7} = \begin{bmatrix} 0 & \frac{\partial_{N5}}{\partial_{\xi}} & 0 & 0 & \frac{\partial_{N6}}{\partial_{\xi}} & 0 \\ 0 & \frac{\partial_{N5}}{\partial_{\eta}} & 0 & 0 & \frac{\partial_{N6}}{\partial_{\eta}} & 0 \\ 0 & \frac{\partial_{N5}}{\partial_{\varphi}} & 0 & 0 & \frac{\partial_{N6}}{\partial_{\varphi}} & 0 \end{bmatrix} \tag{34}$$

$$\mathbf{DN8} = \begin{bmatrix} 0 & \frac{\partial_{N7}}{\partial_{\xi}} & 0 & 0 & \frac{\partial_{N8}}{\partial_{\xi}} & 0 \\ 0 & \frac{\partial_{N7}}{\partial_{\eta}} & 0 & 0 & \frac{\partial_{N8}}{\partial_{\eta}} & 0 \\ 0 & \frac{\partial_{N7}}{\partial_{\varphi}} & 0 & 0 & \frac{\partial_{N8}}{\partial_{\varphi}} & 0 \end{bmatrix} \tag{35}$$

$$\mathbf{DN9} = \begin{bmatrix} 0 & 0 & \frac{\partial_{N1}}{\partial_{\xi}} & 0 & 0 & \frac{\partial_{N2}}{\partial_{\xi}} \\ 0 & 0 & \frac{\partial_{N1}}{\partial_{\eta}} & 0 & 0 & \frac{\partial_{N2}}{\partial_{\eta}} \\ 0 & 0 & \frac{\partial_{N1}}{\partial_{\varphi}} & 0 & 0 & \frac{\partial_{N2}}{\partial_{\varphi}} \end{bmatrix} \tag{36}$$

$$\mathbf{DN10} = \begin{bmatrix} 0 & 0 & \frac{\partial_{N3}}{\partial_{\xi}} & 0 & 0 & \frac{\partial_{N4}}{\partial_{\xi}} \\ 0 & 0 & \frac{\partial_{N3}}{\partial_{\eta}} & 0 & 0 & \frac{\partial_{N4}}{\partial_{\eta}} \\ 0 & 0 & \frac{\partial_{N3}}{\partial_{\varphi}} & 0 & 0 & \frac{\partial_{N4}}{\partial_{\varphi}} \end{bmatrix} \tag{37}$$

$$\mathbf{DN11} = \begin{bmatrix} 0 & 0 & \frac{\partial_{N5}}{\partial_{\xi}} & 0 & 0 & \frac{\partial_{N6}}{\partial_{\xi}} \\ 0 & 0 & \frac{\partial_{N5}}{\partial_{\eta}} & 0 & 0 & \frac{\partial_{N6}}{\partial_{\eta}} \\ 0 & 0 & \frac{\partial_{N5}}{\partial_{\varphi}} & 0 & 0 & \frac{\partial_{N6}}{\partial_{\varphi}} \end{bmatrix} \tag{38}$$

$$\mathbf{DN12} = \begin{bmatrix} 0 & 0 & \frac{\partial_{N7}}{\partial_{\xi}} & 0 & 0 & \frac{\partial_{N8}}{\partial_{\xi}} \\ 0 & 0 & \frac{\partial_{N7}}{\partial_{\eta}} & 0 & 0 & \frac{\partial_{N8}}{\partial_{\eta}} \\ 0 & 0 & \frac{\partial_{N7}}{\partial_{\varphi}} & 0 & 0 & \frac{\partial_{N8}}{\partial_{\varphi}} \end{bmatrix} \tag{39}$$

or in a compact form as:

$$\mathbf{DN} = \begin{bmatrix} \mathbf{DN1} & \vdots & \mathbf{DN2} & \vdots & \mathbf{DN3} & \vdots & \mathbf{DN4} \\ \cdots & \cdots & \cdots & \cdots & \cdots & \cdots & \cdots \\ \mathbf{DN5} & \vdots & \mathbf{DN6} & \vdots & \mathbf{DN7} & \vdots & \mathbf{DN8} \\ \cdots & \cdots & \cdots & \cdots & \cdots & \cdots & \cdots \\ \mathbf{DN9} & \vdots & \mathbf{DN10} & \vdots & \mathbf{DN11} & \vdots & \mathbf{DN12} \end{bmatrix} \tag{40}$$

Based on the equation referring to the deformation vector, it is possible to conclude that:

$$\boldsymbol{\varepsilon} = \mathbf{H} \begin{bmatrix} \frac{\partial_u}{\partial_x} \\ \frac{\partial_u}{\partial_y} \\ \frac{\partial_u}{\partial_z} \\ \frac{\partial_v}{\partial_x} \\ \frac{\partial_v}{\partial_y} \\ \frac{\partial_v}{\partial_z} \\ \frac{\partial_w}{\partial_x} \\ \frac{\partial_w}{\partial_y} \\ \frac{\partial_w}{\partial_z} \end{bmatrix} \tag{41}$$

where the matrix H will be expressed by:

$$\mathbf{H} = \begin{bmatrix} 1 & 0 & 0 & 0 & 0 & 0 & 0 & 0 & 0 \\ 0 & 0 & 0 & 0 & 1 & 0 & 0 & 0 & 0 \\ 0 & 0 & 0 & 0 & 0 & 0 & 0 & 0 & 1 \\ 0 & 1 & 0 & 1 & 0 & 0 & 0 & 0 & 0 \\ 0 & 0 & 0 & 0 & 0 & 1 & 0 & 1 & 0 \\ 0 & 0 & 1 & 0 & 0 & 0 & 1 & 0 & 0 \end{bmatrix} \tag{42}$$

Hence, from Eq. (43):

$$\begin{bmatrix} \frac{\partial_u}{\partial_x} \\ \frac{\partial_u}{\partial_y} \\ \frac{\partial_u}{\partial_z} \\ \frac{\partial_v}{\partial_x} \\ \frac{\partial_v}{\partial_y} \\ \frac{\partial_v}{\partial_z} \\ \frac{\partial_w}{\partial_x} \\ \frac{\partial_w}{\partial_y} \\ \frac{\partial_w}{\partial_z} \end{bmatrix} = \boldsymbol{\Gamma}_u \begin{bmatrix} \frac{\partial_u}{\partial_\xi} \\ \frac{\partial_u}{\partial_\eta} \\ \frac{\partial_u}{\partial_\varphi} \\ \frac{\partial_v}{\partial_\xi} \\ \frac{\partial_v}{\partial_\eta} \\ \frac{\partial_v}{\partial_\varphi} \\ \frac{\partial_w}{\partial_\xi} \\ \frac{\partial_w}{\partial_\eta} \\ \frac{\partial_w}{\partial_\varphi} \end{bmatrix} \tag{43}$$

It is possible to arrive at $\mathbf{\Gamma_u}$, defined by the following relation:

$$\mathbf{\Gamma}_u = \begin{bmatrix} \Gamma(\xi,\eta,\varphi) & \vdots & \mathbf{0} & \vdots & \mathbf{0} \\ \cdots & \cdots & \cdots & \cdots & \cdots \\ \mathbf{0} & \vdots & \Gamma(\xi,\eta,\varphi) & \vdots & \mathbf{0} \\ \cdots & \cdots & \cdots & \cdots & \cdots \\ \mathbf{0} & \vdots & \mathbf{0} & \vdots & \Gamma(\xi,\eta,\varphi) \end{bmatrix} \quad (44)$$

Since the matrix Γ(ξ,η,φ) has 3 rows and 3 columns.The following formatting rules must be followed strictly. This (.doc/.docx) document may be used as a template for papers prepared using Microsoft Word. Papers not conforming to these requirements may not be published in the journal.

2.3 Calculation of von Mises Stress

For elements that are subject to plane stresses, it is possible to inform that the von Mises stress is represented by the following relation, since the yield stress must be greater than the calculated von Mises stress:

$$\sigma_{VM} = \sqrt{\sigma_x{}^2 + \sigma_y{}^2 - \sigma_x\sigma_y + 3\tau_{xy}{}^2} \quad (4545)$$

III. APPLICATION

Two examples will be presented using the implemented computational code. The mechanical properties of the following steels and alloys were used: for the structural carbon steel of medium and high mechanical strength (MS250 and HS350, respectively), the Modulus of Elasticity (E) of 200 GPa and the Poisson coefficient (υ) of 0.3; for stainless steel (SS304), the Modulus of Elasticity (E) of 193 GPa and the coefficient of Poisson (υ) of 0.27 and for the superalloy inconel (SI718), the Modulus of Elasticity (E) of 206 GPa and the Poisson coefficient (υ) of 0.28.
For the yield stress of the materials, the following values were used: 250 MPa and 350 MPa for structural carbon steel of medium and high mechanical strength, respectively; 215 MPa for stainless steel and 820 MPa for inconel alloy.

3.1 Example 1: 4-node tetrahedral element

The example shown in Fig. 2 refers to the modeling of the solid that was discretized with only a 4-node tetrahedral finite element.

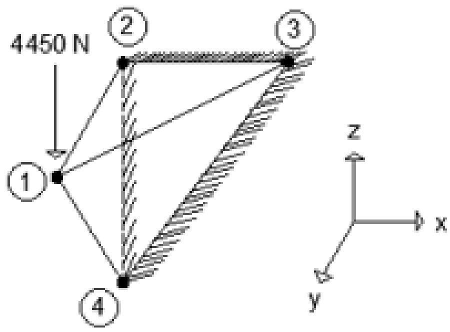

Source: Author
Figure 2 - Example T4

For the analysis of the nodal displacement in the solid above, the coordinates of the nodes, given in millimeters, were defined as:

1 (0.25.25) 2 (0.0.25) 3 (25.0.25) 4 (0.0.0)

In order to validate the developed computational program, Tab. 1 the comparison between the result obtained by the research and that found in the literature.

Table 1 – Comparison of T4 Nodal Displacent in z

Nodes	Present work (mm)	[9] (mm)	Present work / Literatura
1	-0.01341	-0.01340	1.00075
2	0.00000	0.00000	1.00000
3	0.00000	0.00000	1.00000
4	0.00000	0.00000	1.00000

Source: Author

Table 2 presents the results obtained by the implemented code for the materials used in this research.

Table 2 - T4 Nodal Displacent in z

Nodes	MS250 (mm)	HS350 (mm)	SS304 (mm)	SI718 (mm)
1	-0.0139	-0.0139	-0.0141	-0.0133
2	0.0000	0.0000	0.0000	0.0000
3	0.0000	0.0000	0.0000	0.0000
4	0.0000	0.0000	0.0000	0.0000

Source: Author

3.2 Example 2: L-shaped portico (H8)

In this application, a discretized steel frame with four 8-node hexahedral finite elements (H8) was analyzed. The structure was subjected to a point load P = 80 kN at node 4, with E = 200 GPa and υ = 0.3. Fig 3 shows the dimensions of the structure and in Fig 4 it is possible to visualize the discretization used.

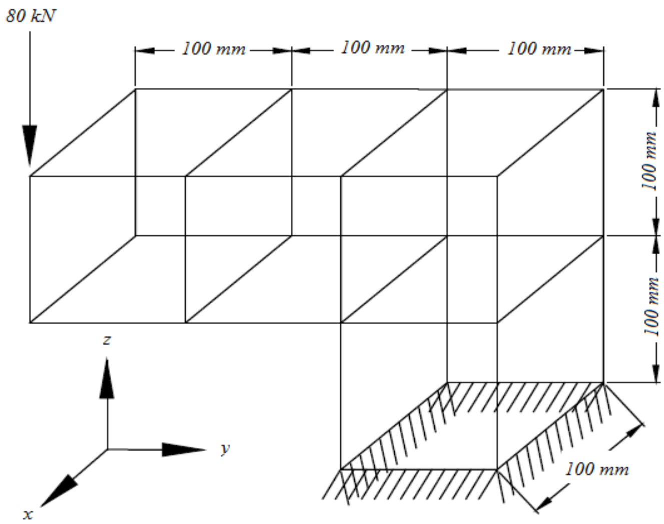

Source: Author

Figure 3 - L-shaped porch – dimensions

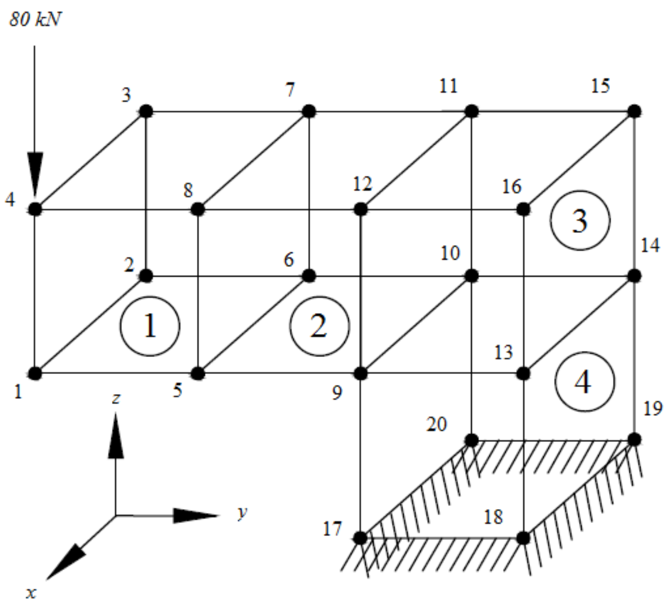

Source: Author
Figure 4 - L-shaped portico – discretization used.

Statically analyzing the structure in question, in Table 3 it is possible to compare the nodal displacements obtained by the present work and the results found in the literature by [9].

Table 3 – L-shaped frame - Nodal displacements in z.

Nodes	Present work (mm)	[9] (mm)	Present work / Literatura
1	-0,40980	-0,409828806	0,999929712
2	-0,33230	-0,33229407	1,000017846
3	-0,32680	-0,326759294	1,000124575
4	-0,42780	-0,427797766	1,000005222
5	-0,22310	-0,223092587	1,000033228
6	-0,16710	-0,167106482	0,99996121
7	-0,16710	-0,167070616	1,000175878
8	-0,21740	-0,21737743	1,000103829
9	-0,04787	-0,047867013	1,000062402
10	-0,02934	-0,029338382	1,00005515
11	-0,03740	-0,037397392	1,000069737
12	-0,06300	-0,063003081	0,999951098
13	0,02909	0,029087101	1,000099666
14	0,03968	0,039684492	0,999886807
15	0,05580	0,055798691	1,000023459
16	0,03958	0,03958274	0,999930778

Source: Author

Table 4 shows the results obtained for the von Mises stresses in each element compared with the results from [9].

Table 4 – Element 1 – Von Mises Stresses.

Strain	Present work (N/mm²)	[9] (N/mm²)	Present work / Literatura
σ_1	23,36000	23,35900	1,00000
σ_2	29,93000	29,92900	1,00003
σ_3	40,58000	40,58200	0,99995
σ_4	43,40000	43,39600	1,00009
σ_5	18,54000	18,54500	0,99973
σ_6	14,85000	14,84900	1,00007
σ_7	15,98000	15,98400	0,99975
σ_8	17,91000	17,91000	1,00000

Source: Author

Table 5 presents the nodal displacements obtained by the present work for the materials under analysis.

Table 5 – L-shaped frame – Analysis of nodal displacements in z.

Nodes	MS250 (mm)	HS350 (mm)	SS304 (mm)	SI718 (mm)
1	-0,40980	-0,40980	-0,43170	-0,40250
2	-0,33230	-0,33230	-0,35270	-0,32810
3	-0,32680	-0,32680	-0,34670	-0,32250
4	-0,42780	-0,42780	-0,45070	-0,42020
5	-0,22310	-0,22310	-0,23560	-0,21950
6	-0,16710	-0,16710	-0,17770	-0,16520
7	-0,16710	-0,16710	-0,17770	-0,16520
8	-0,21740	-0,21740	-0,22950	-0,21380
9	-0,04787	-0,04787	-0,05151	-0,04771
10	-0,02934	-0,02934	-0,03183	-0,02941
11	-0,03740	-0,03740	-0,04009	-0,03717
12	-0,06300	-0,06300	-0,06722	-0,06243
13	0,02909	0,02909	0,03095	0,02877
14	0,03968	0,03968	0,04258	0,03948
15	0,05580	0,05580	0,05946	0,05524
16	0,03958	0,03958	0,04200	0,03907

Source: Author

Table 6 shows the results obtained for the von Mises stresses in each element of the analyzed materials.

Table 6 – Element 1 – Von Mises stresses of the materials under analysis.

Strain	MS250 (N/mm²)	HS350 (N/mm²)	SS304 (N/mm²)	SI718 (N/mm²)
σ_1	23,36000	23,36000	23,16000	23,22000
σ_2	29,93000	29,93000	29,80000	29,84000
σ_3	40,58000	40,58000	40,86000	40,77000
σ_4	43,40000	43,40000	43,63000	43,55000
σ_5	18,54000	18,54000	19,16000	18,96000
σ_6	14,85000	14,85000	14,89000	14,87000

σ_7	15,98000	15,98000	15,97000	15,97000
σ_8	17,91000	17,91000	17,78000	17,82000

Source: Author

IV. Conclusions

It is noteworthy that the computer program developed for the 4-node tetrahedral element, as demonstrated in example 1, revealed nodal displacements with a percentage difference of just 0.00075% compared to the values found in the literature. In the solids examined in this study, it was observed that the smallest nodal displacement occurred in the Inconel 718 superalloy, while stainless steel recorded the largest nodal displacement.

For cases in which the solids were analyzed with hexahedral finite elements of 8 nodes and 20 nodes, the integrals were solved numerically with the aid of the Gauss-Legendre Method (Gauss Quadrature). When evaluating the solids with the materials in question, it was found that, in relation to nodal displacements, the Inconel 718 superalloy presented the lowest value, while stainless steel, in general, recorded the highest displacement value. Additionally, it should be noted that, for structures with curvilinear geometries, the H20 finite element is the most recommended for analysis.

In these analyses, the significant influence of the Modulus of Elasticity and Poisson's Ratio on the resistance capacity of a solid when subjected to a load stands out, showing that the Modulus of Elasticity is inversely proportional to its deformability. This indicates that the higher the Modulus of Elasticity, the lower the deformation of the structure.

In the present research, the von Mises method was used to analyze stresses in all examples. It is concluded that none of the evaluated materials failed, as the von Mises stress values did not exceed the yield stress values of the analyzed materials.

Therefore, it can be concluded that the implementation developed was satisfactory, providing accurate values of stress, strain and displacement for solids subjected to certain types of loading.

REFERENCES

[1] ZIENKIEWICZ, O. C., La Methods' des elements fínits (translated from the English), Pluralis, France, 1976.

[2] GALLAGHER, R. H., Introduction aux elements finis(translated from the English by J .L. Claudon), Pluralis, France, 1976.

[3] ABSI, E., Methode de calcul numérique en elaticité, Eyrolles, France, 1978.

[4] ROCKEY, K.C., Evans,H.R., Griffiths, D.W. and Nethercot, D.A., Elements finis, (translated from the English by C. Gomes), Eyrolles, France, 1979.

[5] IMBERT, J. F., Analyse des structures par elémentsfinis, Cepadues Ed., France, 1979.

[6] ALMEIDA, Marcelo Lucas de. ELEMENTOS FINITOS PARAM´ETRICOS IMPLEMENTADOS EM JAVA. 2005. Dissertação (Mestre em engenharia civil) - Universidade Federal de Minas Gerais, Belo Horizonte, 2005.

[7] MACIEL, Rui Miguel da Costa Alves. Método dos elementos finitos aplicado à análise de sólidos: concepção e implementação. 2013. Dissertação (Mestre em engenharia civil) - Universidade Técnica de Lisboa, [S. l.], 2013.

[8] CHAPMAN, S. J., 2007, “Fortran 90/95 for Scientists and Engineers”, McGraw-Hill, 2nd ed.

[9] CHANDRUPATLA, T.R., Belegundu, A.D., 2012, “Introduction to Finite Elements in Engineering”, 4rd ed. Pearson Education Limited, Edinburgh Gate, Reino Unido.

Authors

Lukerman Douglas de Almeida:
Master in Structures and Construction from the Federal University of Ouro Preto - UFOP
Degree in Civil Engineering from the State University of Minas Gerais - UEMG

Paulo Anderson Santana Rocha:
Doctorate in Civil Engineering, in the area of Structures, from the Alberto Luiz Coimbra Institute for Postgraduate Studies and Research - COPPE - Federal University of Rio de Janeiro.
Master in Structures and Construction from the Federal University of Ouro Preto - UFOP.
Degree in Civil Engineering from the Federal University of Sergipe - UFS.
He works in the field of structures, specifically in computational mechanics and applied mathematics.